Environmental and Experimental Botany 167 (2019) 103832

Contents lists available at ScienceDirect

Environmental and Experimental Botany

journal homepage: www.elsevier.com/locate/envexpbot

Drought tolerance mechanisms and aquaporin expression of wild vs. cultivated pear tree species in the field

Indira Paudel[a,b], Hadas Gerbi[b], Annat Zisovich[c], Gal Sapir[d], Shifra Ben-Dor[e], Vlad Brumfeld[f], Tamir Klein[a,*]

[a] Department of Plant & Environmental Sciences, Weizmann Institute of Science, Rehovot 76100, Israel
[b] Department of Forestry and Natural Recourses, Purdue University, IN, USA
[c] Extension Service, Ministry of Agriculture, Kiryat Shemona, 10200, Israel
[d] MIGAL – Galilee Research Institute, P.O. Box 831, Kiryat Shemona 11016, Israel
[e] Life Science Core Facilities, Weizmann Institute of Science, Rehovot 76100, Israel
[f] Department of Chemical Research Support, Weizmann Institute of Science, Rehovot 76100, Israel

ARTICLE INFO

Keywords:
Wild species
Cultivated species
Water relations
Aquaporin
Drought
Starch

ABSTRACT

Water availability is becoming a limiting factor with increasing world population that challenges global food security. Thus, we need to enhance cultivation in increasingly drier and hotter climate and prepare fruit trees for the ongoing climate change. Wild tree species might offer vital information and plant material in face of these challenges.

A year-long comparative field study was conducted to investigate the mechanisms underlying drought tolerance in pear species (cultivated *Pyrus communis* and *Pyrus pyrifolia* vs. the wild *Pyrus syriaca*).

We confirmed the hypothesis of higher drought tolerance in wild pear compared to its cultivated relative. *P. syriaca* xylem had fewer, narrower vessels, and lower vulnerability to embolism. It showed higher intrinsic water-sue efficiency and more robust seasonal patterns of photosynthesis, hydraulic conductivity, and PIP (plasma intrinsic protein) aquaporin expression. Across species, we identified a ubiquitous gene (PIP1:5/1:6), nine drought-inhibited genes, and two drought-induced genes (PIP1:4 and 2:6/2:7, confirming previous studies).

Our study highlights the potential of using wild relatives of fruit tree species to prepare key crops to a drier and hotter future. The study of PIPs leads the way to a more focused research of the role of these cellular water channels in minimizing tree water loss under drought, while ensuring hydration of specific tissues.

1. Introduction

Over the course of domestication, cultivated tree yields have doubled and tripled, while other traits have been diminished (Feurtey et al., 2017). Of special interest are drought tolerance traits, which become increasingly important in the current climate change scenario. Water deficit causes drought stress across plant tissues as root water uptake is lower than leaf transpiration (Aroca et al., 2012), resulting in a decline in plant growth and productivity. Water availability was identified as the major factor controlling tree growth globally (Klein et al., 2015). Trees have developed many sophisticated mechanisms to survive under drought stress. These mechanisms involve both physical and biological processes operating at the cellular and whole-organism level (McDowell et al., 2008; Klein et al., 2011; Nardini et al., 2011). Two important strategies to cope with drought are (1) the maintenance of hydraulic conductivity and (2) the use of carbon reserves. Native tree species which experience severe periodic droughts tend to have larger safety margins than cultivated species (Pockman and Sperry, 2000), the latter being more efficient in water transport, since requirements for hydraulic efficiency and safety are often contrasting.

Maintenance of hydraulic conductivity involves, among others, stomatal closure under increasing tension (a biophysical process) and changes in the activity of aquaporins, membrane proteins forming cellular water channels (AQPs) (a biochemical process) (Sade et al., 2010, 2014, Brodribb and Holbrook, 2003). During drought stress, stomata close to reduce transpiration. Otherwise, xylem sap tension is likely to reach a critical threshold where air aspirates through pit membranes or gas bubbles spontaneously nucleate from dissolved gas

Abbreviations: NSC, nonstructural carbohydrates; SWC, soil water content; Stem WP, stem water potential; g_s, stomatal conductance; Tr, transpiration; ET, evapotranspiration; Pn, photosynthesis

* Corresponding author.
E-mail address: tamir.klein@weizmann.ac.il (T. Klein).

https://doi.org/10.1016/j.envexpbot.2019.103832
Received 1 May 2019; Received in revised form 9 July 2019; Accepted 26 July 2019
Available online 31 July 2019
0098-8472/

in the xylem sap. Because of the negative pressure inside the xylem conduits, the gas expands, resulting in embolism (Broderse et al., 2013; Brodribb and McAdam, 2017). Once xylem vessels are embolised, they are no longer functional to conduct water, unless they are recovered. However, xylem vessels and pit membranes can alter their structure to avoid embolism. Small pit pores and narrow conduits increase hydraulic safety (Tyree and Zimmermann, 2002).

In addition to the anatomical properties of the xylem, the close association of living xylem conduits and parenchymal cells to dead xylem vessels have been suggested to be involved in recovery from embolism (Almeida-Rodriguez et al., 2012, Paudel et al., 2016; Zwieniecki and Secchi, 2017). In these living cells, the activity of specific water channels named aquaporins (AQPs), that facilitate the movement of water or other small solutes through membranes, must be considered when contemplating how plants tolerate drought. Among Mediterranean *Quercus* and *Pistacia* trees, apoplast resistance to cavitation correlated well with symplast drought tolerance traits such as membrane stability (Vilagrosa et al., 2010). Yet a general pattern linking plant's hydraulic safety with AQP gene expression in response to drought is yet to be resolved. The AQPs are separated into five subfamilies: plasma membrane intrinsic proteins (PIPs), tonoplast intrinsic proteins (TIPs), nodulin 26-like intrinsic proteins (NIPs), small basic intrinsic protein (SIP) and X intrinsic protein (XIP). Aquaporin upregulation is thought to increase membrane permeability to water transport when water is scarce (Paudel et al., 2017). However, downregulation may encourage cellular water conservation (Almeida-Rodriguez and Hacke, 2012). It is probable that maintenance of a proper water status under drought stress requires both increased water transport via AQPs in some tissues, and reduced water transport in others (Jang et al., 2004). For example, in date palm roots, PdPIP1:1 and 1:3 were upregulated at the early stages of drought stress (Degu et al., 2013). Drought-induced signaling of production, trafficking and phosphorylation alter expression level of AQPs and their role in hydraulic safety (Prado et al., 2013). The hydraulic functions of AQPs have been described for leaves (sheath cells) and roots (exodermis and endodermis), however, only a few studies have focused on the stem xylem (but see Almeida-Rodriguez and Hacke, 2012; Gambetta et al., 2013).

The second strategy adapted by plants to cope with drought involves carbon management. At drought onset, plants often continue photosynthesis, growth and accumulation of nonstructural carbon (C). Studies on the tissue concentrations of C reserves in trees growing under mesic conditions suggest that growth and productivity are not limited by photosynthesis. Nonetheless, C reserves are affected by drought mainly due to the organ-specific reactions of tissue C management (McDowell et al., 2008). One of the potential consequences is a phenomenon called mast seeding. Several studies indicate that high fruit loads restrain the vegetative growth of either the fruit-bearing shoot (Han et al., 2011), or the entire tree (Mund et al., 2010), as a result of C starvation. Drought-induced carbon starvation is hypothesized to result from stomatal closure as part of the trees' hydraulic safety margin (the aforementioned first strategy), in turn negatively affecting carbon availability (McDowell et al., 2008).

Many fruit trees, particularly *Pyrus* species *(Pyrus communis* and *Pyrus pyrifolia)* have been growing under Mediterranean climate for thousands of years (Reales et al., 2010). Irrigation is widely used to minimize hydraulic limitation of growth and productivity under tree cultivation, including species of the Rosaceae family (Romero and Botía, 2006; Cochard et al., 2008; Beikircher and Mayr, 2016). However, in natural ecosystems, wild plant populations are adapted to the prevailing climate and soil conditions. *Pyrus syriaca* is a wild relative of the cultivated *Pyrus* species, and is found in a few locations across Israel (Zohary, 1972; Feinbrun-Dothan and Danin, 1991). The observation that drought tolerance varies widely among sympatric species is well known. However, only a few studies on drought tolerance differences among wild and cultivated fruit trees were made. Thus, our comparative study exploits the phylogenetic proximity between the cultivated species and their wild relative, for the identification of physiological and molecular drought tolerance traits. Such findings can be useful for the development of cultivated species that perform better under warmer and drier conditions.

In this project we aimed to study and characterize drought tolerance traits among cultivated pear and its wild relative and the involvement of PIP aquaporins in the response to hydraulic stress. For clarification, by the term 'tree drought tolerance, we refer to the eco-physiological definition, i.e. tree survival and growth, rather than the agricultural definition, which is defined by the yield penalty. Fruit yields were not measured here, and will be measured in a follow-up study. Our research questions were: (1) How does drought affect water relations and hydraulic traits; (2) Are changes in hydraulic conductivity related to the expression levels of the PIP aquaporins; (3) Does loss of hydraulic conductivity relate to xylem anatomical traits; and (4) How does carbon management (photosynthesis, storage and reserve use) change under drought? Among the species we hypothesized that the wild *P. syriaca* has higher drought tolerance than the cultivated relatives, in one of the mechanisms related to the four questions above.

2. Materials and methods

This study is part of a larger research project on the eco-physiology of wild fruit trees of the family Rosaceae which are native to Israel and the Eastern Mediterranean: *Pyrus syriaca*, *Prunus ursina*, and *Amygdalus ramonensis*. The comparative research project tests drought tolerance traits in these tree species and in their cultivated relatives (pear, prune, and almond, respectively), which are grown in orchards at the same locations. The project aims to (1) link between carbon and water relations traits and tree performance through variations among closely related species; (2) test the potential of using wild tree species as rootstocks for the commercial fruit trees; and (3) promote the conservation of the wild species in their natural habitats, threatened by rapid changes in climate and land-use.

2.1. Experiment setup and plant material

To study the seasonal dynamics of the water relations of pear trees, a field experiment was conducted on adult trees of three pear species. The experiment was performed during August 2017-April 2018 in two sites in the upper Galilee region of Israel: an orchard at the Matityahu Research Station ($33^0$06' 58.11"N; 35^0 45' 27.90"S, 680 m.a.s.l.) and a neighbouring natural maquis site ($33^0$11' 50.43"N; 35^0 33' 17.97"S, 510 m.a.s.l.). The Matityahu Research Station is located adjacent to the village of Bar'am, bordering Lebanon, at the heartland of the upper Galilee orchard country, which produces the majority of pear, apple, and additional crops for the Israeli fruit market. *Pyrus communis* and *P. pyrifolia* trees were planted in 2009 and 2010, respectively, and were 3 m tall at the time of measurement. *P. syriaca* trees were 2–3 m tall, and older than 10 years, but there was no exact information about their age. All measurements and samples were taken at middle-top crown height of 1.5–3 m. The sites are only ˜20 km apart, at similar elevation, and are part of the same geographical region. The climate is typically Mediterranean with a mild wet season in winter and a hot and dry summer. Mean annual precipitation is 550 mm, typically restricted to November-April. Meteorological data for the study period were downloaded from the Ministry of Agriculture meteorological station at the research station, and from the Israel Meteorological Service station in Kfar Giladi, 5 km NE of the maquis site. At both sites, six trees from each species, two cultivated species (*Pyrus communis, Pyrus pyrifolia*) and a wild species (*Pyrus syriaca*) were selected. *Pyrus syriaca* is the only pear species native to the Eastern Mediterranean, where it is not a common tree. Its fruits are smaller than those of its cultivated relatives, yet edible. *Pyrus communis*, the European pear and *Pyrus pyrifolia*, the Asian pear, are the two major commercial pear species, grown in

Europe, North America and Australia, and in East Asia, respectively. The study trees were growing in heavy clay soil. Cultivated and wild trees were 3.5–4 m and 3–6 m tall with stem diameter at 10 cm above ground of 16 ± 4 cm and 17 ± 8, respectively. Cultivated trees received irrigation all year round, except in winter when there was enough rainfall. To allow comparison between cultivated and wild species, a drought period was imposed on six trees of each cultivated species, by withholding irrigation between end of August and early October in 2017. Trees were healthy with no visible signs of biotic or abiotic stress. Measurements were performed on all trees at each of seven measurement days: once before the dry-down cycle, twice during the dry-down, and four times following winter to spring seasons. For some of the parameters there were 1–2 additional drought or post-drought measurement days.

2.2. Soil water conditions

Soil water content on volumetric basis (SWC, % v/v) was measured using a dielectric constant EC-10 soil moisture sensor (Decagon Devices Inc., Pullman, WA, USA). Measurements were performed 20–40 cm away from the tree stem, and at 10 cm soil depth, at each field measurement day. To correct for sensor bias, sensor readings in heavy clay were calibrated against measured SWC in the standard oven drying procedure using an additional soil batch. The correlation between sensor readings and true SWC yielded a linear relationship, yet with a roughly constant 6.5% underestimation by the sensor ($R^2 = 0.97$, $0 < SWC < 45\%$ v/v), and the sensor readings were corrected accordingly.

2.3. Stem water potential

Stem water potential (stem WP) was measured at midday on leaf cohorts sampled from 4 to 6 randomly selected trees per treatment. This parameter was chosen as a key proxy for drought tolerance, since it integrates leaf- and stem-level responses, as observed in our previous drought experiment on young lemon trees (Paudel et al., 2018). Leaves were covered at least 40 min before taking measurements, to allow equilibration between the leaf tissue and the stem xylem. Stem WP was measured on the same branches as used for gas exchange, hydraulics and non-structural carbohydrate measurements. Following cutting, Stem WP was measured within 2 min of collection using a Scholander-type pressure chamber (PMS Instrument Company, Albany, OR, USA).

2.4. Xylem hydraulic conductivity

Three branch segments of 75 cm each were cut under water from each tree, according to protocols adjusted from Sperry et al. (1988) and Wheeler et al. (2013). Branch length was chosen according to the most abundant vessel length across the related *Prunus* species (Cochard et al., 2008). Branches were placed under water during transportation to the lab (about 2.5 h) in order to allow relaxation of the xylem tension. Next, the segments were further cut under water in the lab from two edges into the final measured size of 10 cm. Xylem conductivity was measured with a 70 cm column of water (7 kPa) in order to capture the native hydraulic conductivity (Ks-native). The same segments were then flushed with 19 mM KCl aqueous solution a High-Pressure Flow Meter (Dynamax Inc., Texas, USA; Tyree et al., 1995) for 20 min at pressures of 0.05-0.1 MPa to calculate the percentage loss of hydraulic conductivity (PLC), as an indirect measurement of embolism. Correlations of PLC by stem WP were made for each of the species, yielding empiric vulnerability curves. To create these curves, data were uploaded to JMP (Carey, NC, USA), where the 'fit curve' function was applied. We registered stem WP as the regressor, PLC as the response, and grouped by species. In addition, all curves were forced to (0 MPa, 0%), and to (-10 MPa, 100%). The first point indicates that no embolism is expected at a stem WP of zero. The second point is a preliminary, rough, estimate of a stem WP value where 100% embolism is highly likely to occur. Since the maximum PLC value in our dataset was only 37%, we needed to rely on an external dataset. In a survey of ten species of the related genus *Prunus*, PLC of 90–100% was measured at a stem WP value of -8 MPa (Cochard et al., 2008). The value of -10 MPa was hence chosen as safe to assume 100% PLC for the three *Pyrus* species. Sigmoidal curves were produced according to the Equation:

$$PLC = \frac{100}{1 + \exp(a(\Psi_x - b))} \quad (1)$$

where a and b are the empiric parameters for the curve's growth rate and inflection point, respectively. The fit of each curve to the data was tested using the Chi Square test in JMP.

2.5. Aquaporin gene definition

Among the five AQP families, we chose to study the PIP genes, which, so far, have been studied more intensively than the other AQP families. This was important, since little is known on any AQP family in trees. In addition, our study built on the findings of Paudel et al. (2017), who linked downregulation of PIP genes to reductions in root hydraulic conductivity in *Citrus*. The PIP aquaporins were defined from various sources of pear (*Pyrus communis*) sequence. The *Arabidopsis* thaliana PIP protein sequences were used as input to local TBLASTN searches run against the built (Pyrus_communis_v1.0-mRNA_hybrid.fna) and predicted (Pyrus_communis_v1.0-mRNA_augustus.fna) genes from GDR (https://www.rosaceae.org/organism/Pyrus/communis), and against EST sequences (pear_RNA_EST.scafSeq; from http://peargenome.njau.edu.cn/). TBLASTN was also run at NCBI against the TSA database, limited to sequences from *Pyrus communis*. The EST and TSA sequences were clustered to form longer sequences, and then the sequences from the four sources (hybrid, augustus, EST and TSA) were aligned to form non-redundant gene clusters. Each gene cluster was then aligned individually, and the best sequence was chosen. These sequences were compared to the *P. communis* genome, and several of them were improved based on genome sequence. The final set of genes comprised 6 putative PIP1 and 8 putative PIP2 genes. Two of the PIP1 and one of the PIP2 sequences were incomplete. DNA and protein sequences are provided in Table S1. The sequences were then aligned to the PIP aquaporins from various species in order to name them. A final alignment of *Arabidopsis*, Strawberry (*Fragaria vesca*, taken from Deshmukh et al., 2015) and the pear sequences was representative, and was used for the phylogenetic trees. *Arabidopsis* was chosen as the best reference for plant AQPs. Strawberry was chosen because it currently has the best defined collection of AQP genes in the Rosaceae family. For example, peach (*Prunus persica*) and apple (*Malus domestica*) had fewer, or unresolved, AQP genes than strawberry. Multiple alignment was performed using ClustalW 2.1 and phylogenetic trees were constructed with Neighbor Joining in ClustalW2.1, Maximum likelihood with ProML in the Phylip package and PhyML online with the default parameters. The topology of the trees were the same, and the PhyML tree is shown.

2.6. Aquaporin mRNA expression

The transcription level of PIP AQPs was measured in RNA extracts taken from branch wood tissue sampled on 25 September 2017 and 17 January 2018. On these dates, both field and orchard conditions were at the driest and wettest conditions of the study period, respectively. Total RNA was extracted from approximately 200 mg of branch sapwood tissue using the CTAB extraction method. RNA was treated with RQ1 RNase-free DNase (Promega, Fitchburg, WI, USA) according to the manufacturer's instructions. RNA quantity was analyzed in a NanoDrop ND-1000 Spectrophotometer (Wilmington, DE, USA) and RNA quality was determined by Agilent Bioanalyzer (Santa Clara, CA, USA). Next, cDNA was synthesized from 1 µg RNA using OligoT as a primer and M-

MLV Reverse transcriptase (Fermentas, Burlington, Ontario, Canada) in a final volume of 25 µl containing the commercially supplied buffer. Primers were designed based on the defined gene sequences, using the central region present in all of the sequences, using the program Oligo 7, version 7.60 (Molecular Biology Insights, Inc. Colorado Springs, CO, USA. Primer sequences are in Table S2. Real-time PCR was carried out in a reaction mix containing 2 mM gene-specific forward and reverse primers, 3 µl cDNA (diluted 1:5), KAPA SYBR FAST qPCR Master Mix Universal (KAPA Biosystems, Boston, MA), and Ultra-Pure water (Fisher Biotech, Wembley, Australia) in a final volume of 12 µl in a Corbett Rotor-Gene 6000 (Qiagen, Venlo, The Netherlands). Reactions were run for 40 cycles of 10 s at 95° C, 15 s at the annealing temperature for each gene, 20 s extension at 72 °C, and the threshold level was determined. Standard curves were generated for each gene using serial cDNA dilutions. The relative concentration of the product was calculated by the algorithm of the Rotor-Gene software using the CT value. Relative CT method was used to quantify *Pyrus communis* PIPs mRNA transcript levels. Relative expression (RE) was defined as the ratio between the relative concentration of each gene and that of β-actin.

2.7. Xylem embolism and anatomy

Xylem vessels were visualized in two complementary techniques: (1) microCT scans, and (2) light microscopy. MicroCT is an X ray microscopic method based on obtaining cross sections of a sample under different angles of rotation. A complete set of cross sections taken over 180^0 or 360^0 is used for the reconstruction of a full 3D image of the sample. The 3D image can be sectioned at convenient angles providing data on different densities in the sample. This allows to differentiate between air-filled conduits and water-filled conduits in the xylem tissue. Segments for scans were taken from the same branches used for the hydraulic measurements. The samples were cut after xylem relaxation has been completed, and the middle part of the sample was scanned. The measurements were done on a Zeiss Xradia micro XCT 400 instrument (Zeiss X ray microscopy, Peasanton CA, USA) under source voltage of 40 KV and current of 200 µA. In order to reconstruct the volume of the branch,1500 images were taken over 180 degrees, with a voxel size of 2.6 µ m. Reconstruction was made with a proprietary software of Zeiss X ray microscopy which uses a back projection algorithm. The reconstruction was adjusted for maximum light intensity of 0.022782 photons (represented as white pixels) and a minimum intensity of 0.0079 photons (represented as black pixels). In addition, anatomical analyses were conducted on the lower/proximal part of the segments following standard protocols (von Arx et. al., 2016). Entire cross-sections of 10–12 µm thickness were cut with a rotary microtome (RM2245, Leica, Heidelberg, Germany). Sections were stained with safranin and astra-blue (1% and 0.5% in distilled water, respectively), permanently fixed with Eukitt (BiOptica, Milan, Italy), and then photographed using a digital automated light microscope (D-sight, Menarini Diagnostic, Florence, Italy). Images were analyzed using ROXAS v3.0.31 (von Arx and Dietz, 2005; von Arx and Carrer, 2014; Prendin et al., 2017) for the following xylem anatomical features: (1) total xylem area, and (2) mean number of tracheids.

2.8. Leaf gas exchange

Synchronously, prior to stem water potential measurements, leaf CO_2 and H_2O gas exchange measurements were done on young matured leaves using a Walz photosynthesis systems (GFS-3000, Walz, Germany) equipped with a standard 2 × 3 cm leaf cuvette. Measurements were performed at ambient leaf temperature of 25° C, 50% relative humidity, photosynthetically active light intensity of 1200 µmol m^{-2} s^{-1}, 10% blue light, and 400 µmol CO_2 mol^{-1}. Three leaves were measured from each of six trees. These measurements were performed periodically throughout the seasons around midday, i.e. between 10:00 to 14:00. Finally, intrinsic water-use efficiency was calculated as the ratio between photosynthesis and stomatal conductance.

2.9. Non-structural carbohydrate concentration

Plant materials for nonstructural carbohydrate (NSC) analysis were sampled from the same branches used for other measurements, during eight measurement days. Immediately after sampling, all plant materials were subject to a 30 s heat shock using a microwave in the nearby farmhouse facility. In the laboratory, samples were dried at 60 °C to weight constancy in a drying oven (Heratherm Ovens, Thermo Fisher Scientific, MA, USA) and ground using a ball mill (Retsch, Hann, Germany) at a frequency of 25 tilts s^{-1} until tissues had turned into fine powder (~5 min). NSC analyses followed the method by Wong (1990), modified as described in Hoch et al. (2002). Dried wood powder (8–12 mg) was extracted with 2 ml deionized water at 100 °C for 30 min. An aliquot of each sample extract was taken for the determination of low molecular weight carbohydrates using invertase (from baker's yeast; Sigma-Aldrich, Buchs, Switzerland) to break sucrose into glucose and fructose. Glucose and fructose were converted into gluconate-6-phosphate using glucose hexokinase (Sigma Diagnostics, St Louis, MO, USA) and phosphogluconate isomerase (from baker's yeast; Sigma-Aldrich). The total amount of gluconate-6-phosphate was determined as the increase in NADH + H+ using a photometer (HR 700; Hamilton, Reno, NE, USA). For starch determination, the remaining extract was incubated at 40 °C for15 h with amyloglucosidase (from Aspergillus niger; Sigma-Aldrich) to break starch into glucose. NSC was determined as the total amount of glucose as described above. Starch content was calculated as total NSC minus free sugars. All concentrations were calculated on a % dry matter basis.

2.10. Statistical analysis

Leaf gas exchange, stem water potential, soil water content, and non-structural carbohydrates data were each analyzed using a repeated-measurements analysis of variance (ANOVA) with species and drought treatments as fixed factors, assuming that the variance within subjects (i.e., the trees) was homogeneous. For all analyses, there were six replicates of all treatments. Effects of species and drought treatments and their interaction were tested statistically at the drought period, and after recovery time using two-way ANOVA. When effects of treatments were statistically significant, differences among groups were post hoc tested with Tukey's HSD test. All analyses were performed in JMP (SAS, Cary, NC, USA).

3. Results

3.1. Meteorological conditions in the study sites in 2017–2018

During the course of the study period, the climate was typical of the region, and similar across the two sites. Mean daily temperature fluctuated around 10 °C and 30 °C at the peaks of the wet and dry seasons, respectively (Fig. 1). Rainfall occurred between October 2017 and May 2018, with the largest inputs in January-February, up to 42 mm day^{-1}, and higher relative humidity in this period. Conditions close to the native maquis site (Fig. 1a) were slightly cooler and drier than those measured at the orchard farm (Fig. 1b). Specifically, rain events were typically 5–10 mm smaller in magnitude, and temperatures were 3–9 °C lower at the native site.

3.2. Soil moisture and stem water potential

Stem water potential is a good proxy for tree water status across species and along seasons. The three pear species reached minimum values during September-October, which was also the end of the experimental drought period (Fig. 2a). Stem WP increased back to maximum levels in spring, yet the dynamics diverged between the wild and

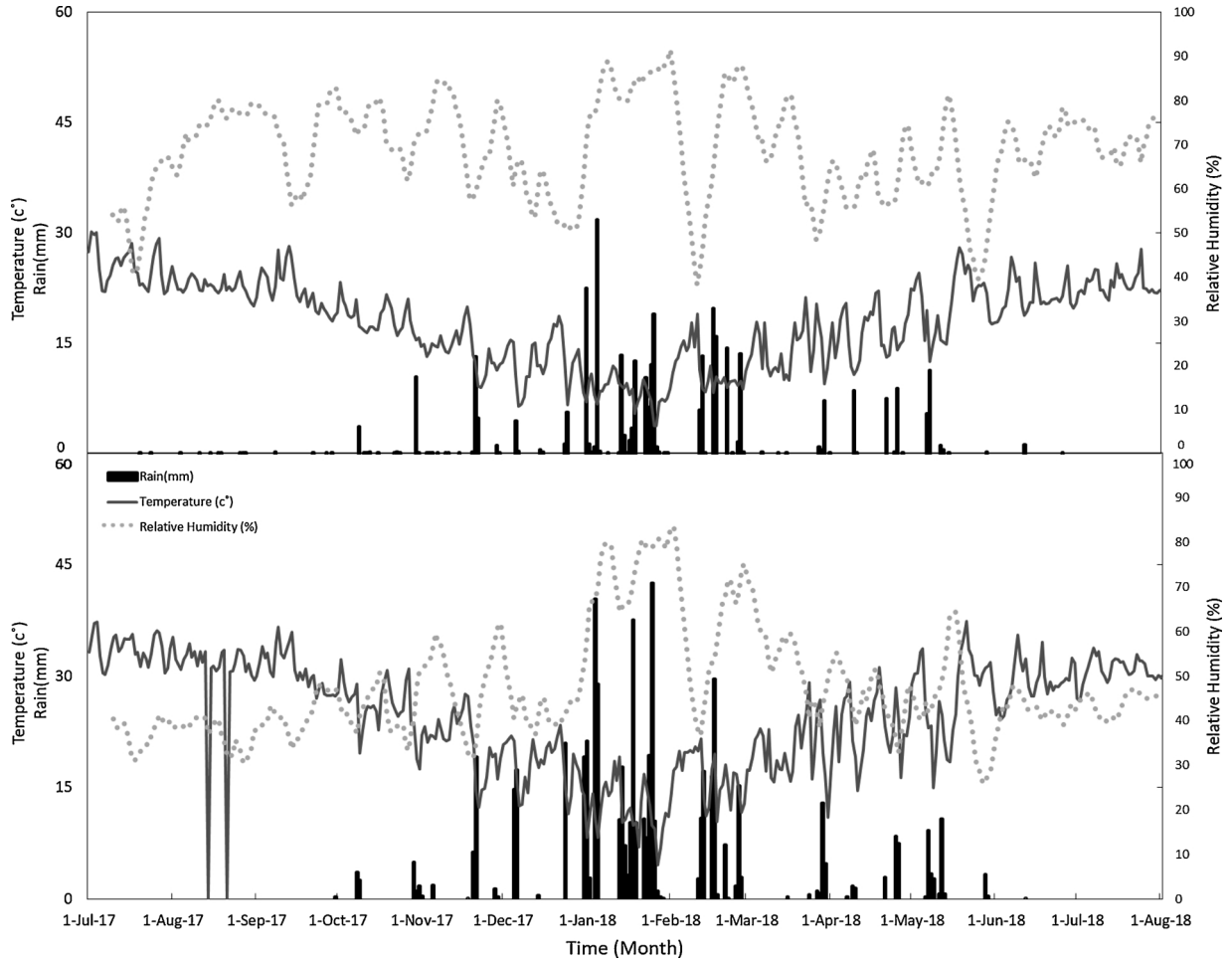

Fig. 1. Meteorological conditions at Matityahu Research Station, by the pear orchard (a) and Kfar Giladi (b), 5 km NNE of the wild pear, native site, during July 2017-July 2018: daily precipitation (mm); Temperature (°C); Relative Humidity (%).

the cultivated species. Winter stem WP was stable around −1.3 MPa among species, dropping under drought to −2.8, −2.6, and -3.8 MPa in *P. communis*, *P. pyrifolia, and P. syriaca,* respectively (Fig. 2a, Table 1). Recovery of *P. syriaca*'s WP was observed after the first significant rainfall at the beginning of November, but was still about 2 MPa below that of its cultivated relatives, which benefitted from the irrigation. In spring, *P. communis* and *P. syriaca* had significantly lower stem WP than *P. pyrifolia* (Fig. 2a). During the summer/drought period, stem WP of *P. syriaca* was significantly lower than that of the cultivated species. Among the two cultivated species, stem WP of *P. communis* was significantly lower than at the end of drought that of *P. pyrifolia*. Soil water content (SWC) reached a minimum of 8% (v/v) during September/end of drought (Fig. 2b). In *P. syriaca*, we observed the expected increase in SWC in the wet season, reaching 28% (v/v) at both the beginning and the end of the wet season. In the orchard, irrigation proved efficient, reaching close to field capacity (40% v/v) in *Pyrus pyrifolia* before the drought, and rapidly recovering from the imposed drought in *Pyrus communis*. Across winter, spring, and September/drought there were no significant differences in SWC among the species.

3.3. Identification of PIP aquaporins in the Pyrus genome

To identify *Pyrus* PIP members, PIP sequences were identified from the *Pyrus communis* transcript sequences and genome annotation by performing TBLASTN using *Arabidopsis* sequences as queries. Based on the *Pyrus* sequences, fourteen members of the PIP gene family were identified. Phylogenetic analysis of the *Pyrus* sequences along with their *Arabidopsis* and strawberry counterparts revealed separation into two clear clades, six genes showing homology with the *Arabidopsis* PIP1 gene family (named hereafter PcPIP1:1–6; Fig. 3 top clade) and eight genes showing homology with the PIP2 gene family of *Arabidopsis* (named hereafter PcPIP2:1–8; Fig. 3 bottom clade). In our sequences, differential primers between PcPIP1:5 and PcPIP1:6, and PcPIP2:4 and PcPIP2:5 could not be designed.

3.4. Hydraulic conductivity and PIPs mRNA expressions

Across species and along seasons, stem hydraulic conductivity (Kh) fluctuated between 1 and 3 g MPa^{-1} s^{-1}. Kh of the cultivated species was significantly affected by drought during the summer (Fig. 4a; Table 1), gradually decreasing as drought progressed. In contrast, *P. syriaca's* hydraulic conductivity reached a minimum in mid-summer and increased continuously throughout the fall. The seasonal dynamics of Kh was significantly different among species (*P. pyrifolia* > *P. communis* > *P. syriaca*) except for the end of the drought period, when species showed similar patterns (Fig. 4a, Table 1). To shed light on the regulation of water transport in the xylem tissue, we further analysed the changes in expression levels of membrane water channels among species and seasons.

Real-time PCR was used to examine the expression of PIP1 and PIP2 gene families in the stems of all species during summer/drought and winter/recovery (Fig. 4b). Overall, several major patterns were observed: (1) transcript levels of PIP 1:5/1:6 were consistently much higher than those of the other family members, regardless of the season/treatment, and accounting for a large portion of the total PIP transcripts in the woody tissue. Inversely, transcripts of PIP2:3 and

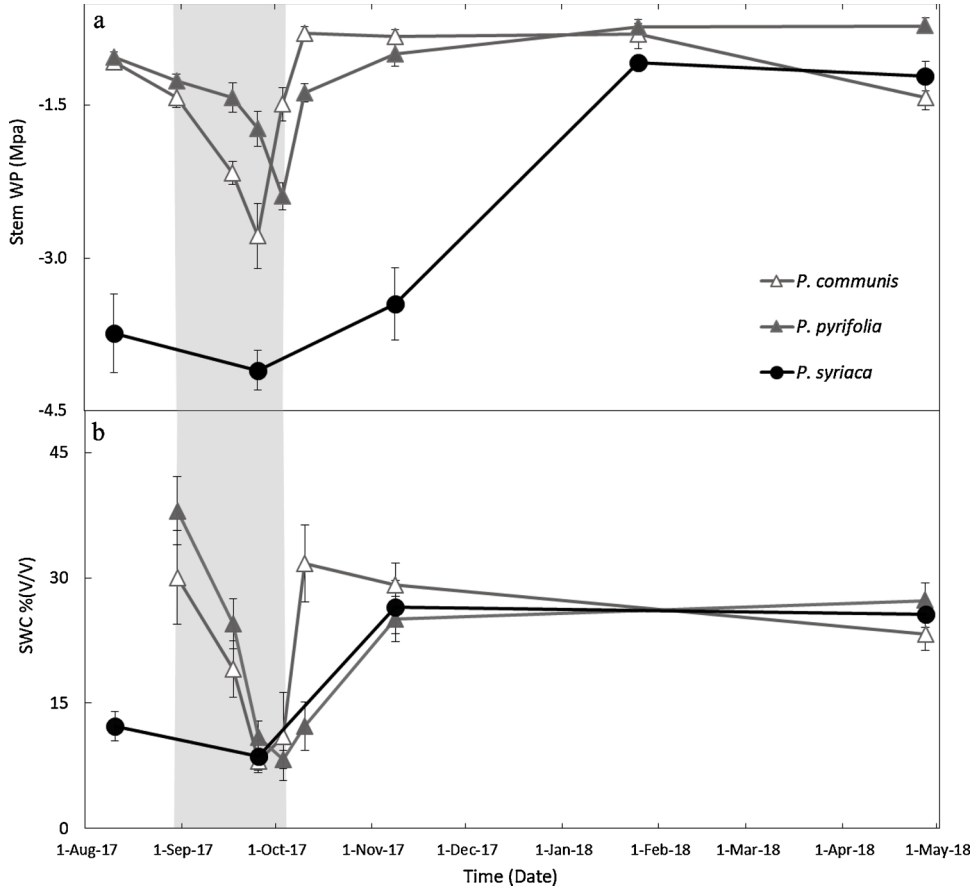

Fig. 2. Stem water potential (a) and soil water content (b) around pear trees through the seasons. Shaded area denotes the 35 days of drought imposed on cultivated trees (*Pyrus communis* and *Pyrus pyrifolia*). Error bars denote the standard error of the mean ($n = 6$). See Table 1 for statistical analysis.

Table 1
P values (probability > F, an effect is significant if P < 0.05, in bold) from ANOVA for species and season (drought/summer vs wet/winter period) in three pear species.

Observed traits	Parameters	Species	Season	Species*Seasons
Water relations	SWC	**0.020**	**0.002**	**0.002**
	Stem WP	**0.003**	**0.000**	**0.003**
Leaf physiology	Tr	**0.045**	**0.002**	**0.001**
	Pn	**0.002**	**0.002**	**0.020**
	gs	**0.004**	**0.001**	**0.034**
Hydraulic traits	Kh Native	0.600	**0.045**	**0.047**
	Kh max	0.200	0.200	2.000
	PLC	0.310	**0.034**	**0.003**
Non-structural carbohydrates	stem-sugar	0.200	**0.045**	0.070
	stem-starch	**0.045**	0.560	0.650
	root-sugar	0.560	**0.003**	0.760
	root-starch	**0.034**	**0.030**	0.650
Plasma membrane proteins	PIP1:1	0.300	**0.010**	**0.030**
	PIP1:2	0.400	**0.020**	**0.020**
	PIP1:3	**0.040**	**0.030**	0.210
	PIP1:4	0.340	**0.023**	**0.030**
	PIP1:5/1:6	**0.002**	**0.000**	**0.030**
	PIP2:1	**0.002**	0.055	**0.001**
	PIP2:2	**0.004**	0.067	0.070
	PIP2:3	0.450	0.540	0.870
	PIP2:4	**0.002**	**0.001**	**0.003**
	PIP2:5	0.670	**0.001**	**0.003**
	PIP2:6/2:7	0.560	0.054	0.056
	PIP2:8	**0.040**	0.054	0.056
Xylem anatomical traits	Vessel density	**0.040**	–	–
	Vessel diameter	**0.001**	–	–

PIP2:4 were nearly non-existent. (2) Transcription levels diverged more among PIP family members than among tree species; yet significant inter-specific differences were identified for some of the genes (Table 1). And (3) Most PIP genes were downregulated during summer/drought compared to winter/recovery; yet other patterns were also observed. PIP1:1, 1:2, 1:3, and 2:5 were downregulated to a similar level among species during summer/drought. Interestingly, PIP1:1, 1:2, and 1:3 transcripts were still rather high in summer in *P. syriaca* (Fig. S1). PIP2:1, 2:2, 2:4 and 2:8 were all rather neutral during winter/recovery, and were strongly downregulated during summer/drought. Of special interest were PIP1:4 and PIP2:6/2:7, which demonstrated unique dynamics. Unexpectedly, the two PIP genes were mildly (PIP2:6/2:7) or strongly (PIP1:4) upregulated during drought. Inter-specific differences were not restricted to those between *P. syriaca* and the cultivars (in PIP1:1, 1:2, and 1:3 above), but included differences in other PIPs (Table 1). In common to these other inter-specific variations is a milder response in *P. communis* compared to that of *P. pyrifolia* and *P. syriaca*.

3.5. Xylem embolism and xylem anatomy

All species showed a drought-induced increase in loss of hydraulic conductivity (PLC), from < 10% in January to ˜25% in summer (Fig. 5). Re-irrigation decreased PLC in the orchard, while PLC of *P. syriaca* in the field increased slightly further. Interestingly, the hierarchy reversed in mid-winter, with only the wild species having PLC < 5%. The rate of embolised vessels was visualised using microCT scans (Fig. 5b), confirming the zero, mild, and moderate levels measured indirectly. Fitting the correlations between stem WP and PLC among the species revealed three species-specific sigmoidal curves of xylem vulnerability

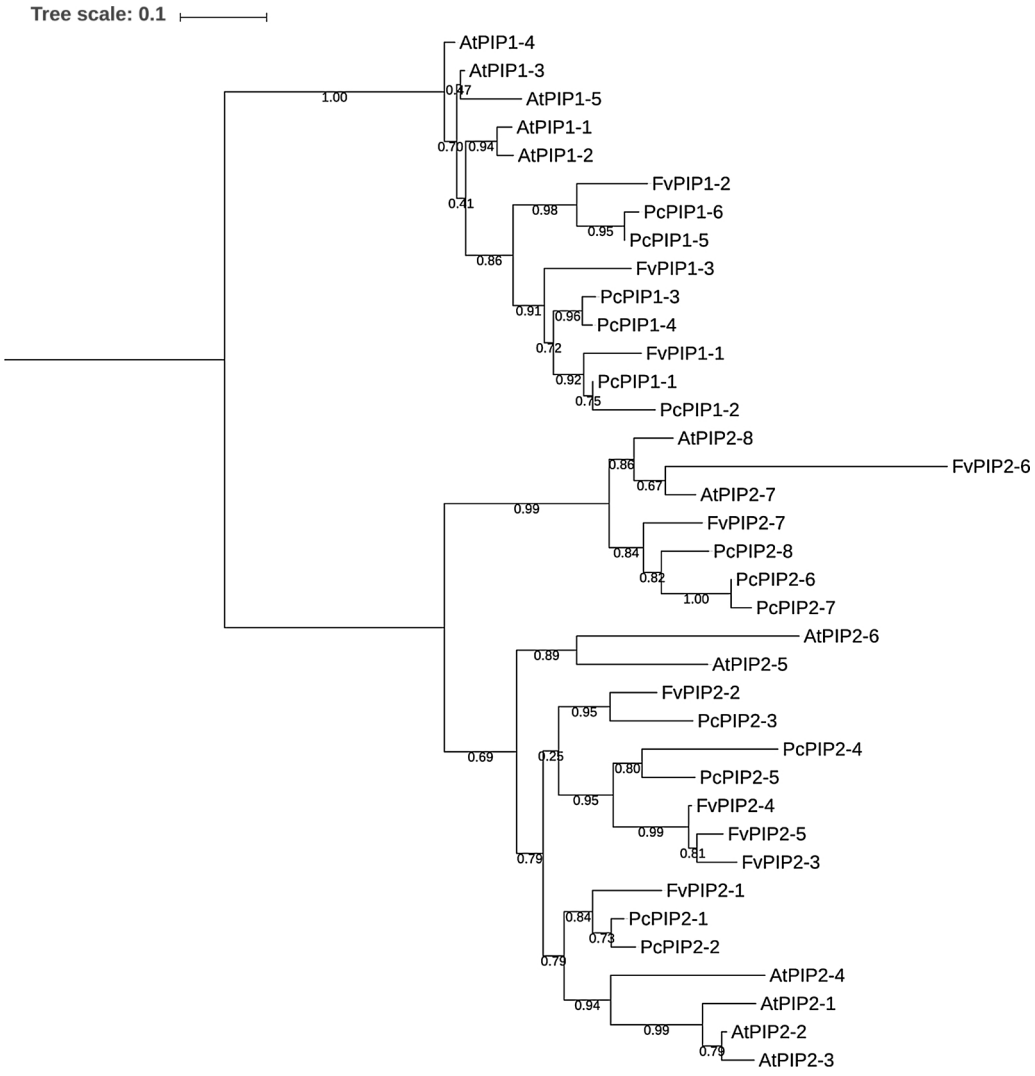

Fig. 3. Phylogenetic tree of *Pyrus communis* (Pc), *Arabidopsis thaliana* (At) and *Fragaria vesca* (Fv) PIP1 and PIP2 aquaporins. The tree was constructed using PhyML.

to embolism (Fig. 5c). The three curves fitted the data-points significantly, yielding the expected vulnerability equations (Table S3). Among the species, xylem vulnerability to embolism was higher for the two cultivated than the wild species, with 50% embolism expected at -4.3 MPa and-6.4 MPa, respectively. Analysis of xylem anatomy revealed small, yet significant, differences among the tree species (Fig. 6; Table 1). Vessel diameter was significantly lower in *P. syriaca* than *P. communis*, in turn lower than in *P. pyrifolia* Vessel frequency was significantly higher in *P. communis* than in *P. pyrifolia* and *P. syriaca*. Overall, the conductive xylem area was significantly lower in the wild vs. the cultivated species, the result of both narrower and fewer vessels.

3.6. Photosynthesis and transpiration

The coupling between CO_2 and water gas exchange in the leaf, and the similar leaf physiology among species, yielded similar species and seasonal patterns between photosynthesis and transpiration (Fig. 7). During summer, *P. pyrifolia* showed the highest activity, and *P. communis* the lowest activity. In spite of the harsh summer conditions, photosynthesis and transpiration were still rather high in *P. syriaca*, and even higher than in its irrigated relative *P. communis*. In addition, by the end of the wet season, the wild pear was slightly more active than its cultivated relatives. Species and season differences were all highly significant (Table 1). Intrinsic water-use efficiency was 2-3-fold higher in the wild vs. the cultivated species during most of the year (Fig. 7c). This large difference was driven by the lower stomatal conductance of the wild species, as a response to the higher temperature and lower relative humidity in the native site compared to the orchard (Fig. 1).

3.7. Wood non-structural carbohydrate dynamics

Levels of branch soluble sugars and starch changed significantly with time (Fig. 8; Table 1). Similar trends were observed in roots (not shown; Table 1). Across the three species, both sugars and starch increased in the wet season, and decreased in summer and under imposed drought. The exception was *P. pyrifolia* starch levels in spring, which were as low as under drought. The decrease in starch levels in spring was ubiquitous, and probably reflected phenological changes, i.e. the production of new leaves and fine roots in spring. The parallel increase in tissue sugars, shortly after the new leaf emergence, means that at least part of this sugar originated from starch breakdown. Among species, non-structural carbohydrates levels were usually higher in *P. communis*, and lower in *P. syriaca*. Divergence from the above trends was observed in three instances: (1) Shoot soluble sugar of *P. syriaca* decreased less following summer/drought (from 0.5% to 1.9% d.m.), compared to the cultivated species (Fig. 8a); (2) A significant reduction in shoot starch in *P. syriaca* (from 8% to 3.7% d.m.), yet well recovered in spring (Fig. 8b) and (3) the relative ratio of sugar fluctuations were higher in cultivated species than in *P. syriaca*. Plotting starch levels against net assimilation (A) yielded a significant linear relationship for

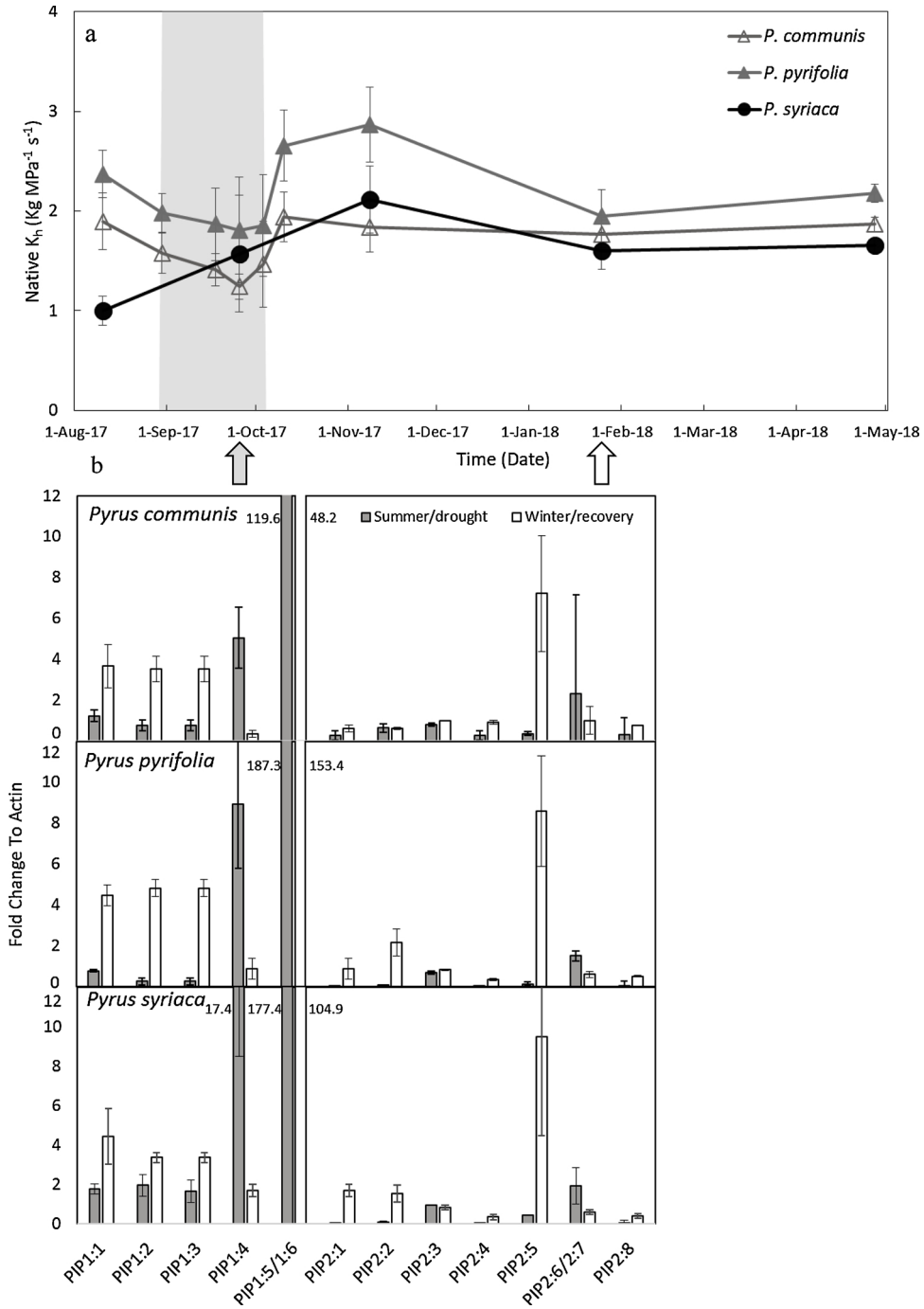

Fig. 4. Native hydraulic conductivity (K_h; a) and aquaporin's PIP gene expression relative to a housekeeping gene (Actin) in summer/drought period and winter/recovery period (b). Values are shown only for transcript levels exceeding the y-axis values. Arrows in panel (a) represent the respective dates in which the expression analyses were performed.

P. syriaca, but not for the cultivated species (Fig. 8c). In the wild species, starch concentration was > 6% d.w. when A was > 5 μmol m^{-2} s^{-1}, and < 4% d.w. when A was < 5 μmol m^{-2} s^{-1}. No such relationship was observed between soluble sugars and A, but since starch was the dominant fraction in NSC, this relationship carried over to the total NSC (data not shown).

4. Discussion

We present a field experiment on physiological drought tolerance mechanisms, also investigating aquaporin dynamics at the molecular level, in two cultivated species and a wild species of the pear tree. The novel aspects of this study are: (1) a detailed comparison between wild and cultivated crop species. Although frequently mentioned in the literature, such a comparison is rarely tested in trees (Schröder and Prasse, 2013); (2) a detailed comparison between the two major cultivars of a fruit tree species. To the best of our knowledge, this is the first comparative study of drought tolerance in *P. communis* and *P. pyrifolia*; (3) aquaporin gene expression dynamics in woody tissues. So far, studies have been investigating aquaporins in leaf, flower bud, and fruit tissues; (4) investigation of aquaporin dynamics in relation with hydraulic conductivity under drought. Although circumstantial evidence, the link is important.

There were clear interspecific differences in water relations,

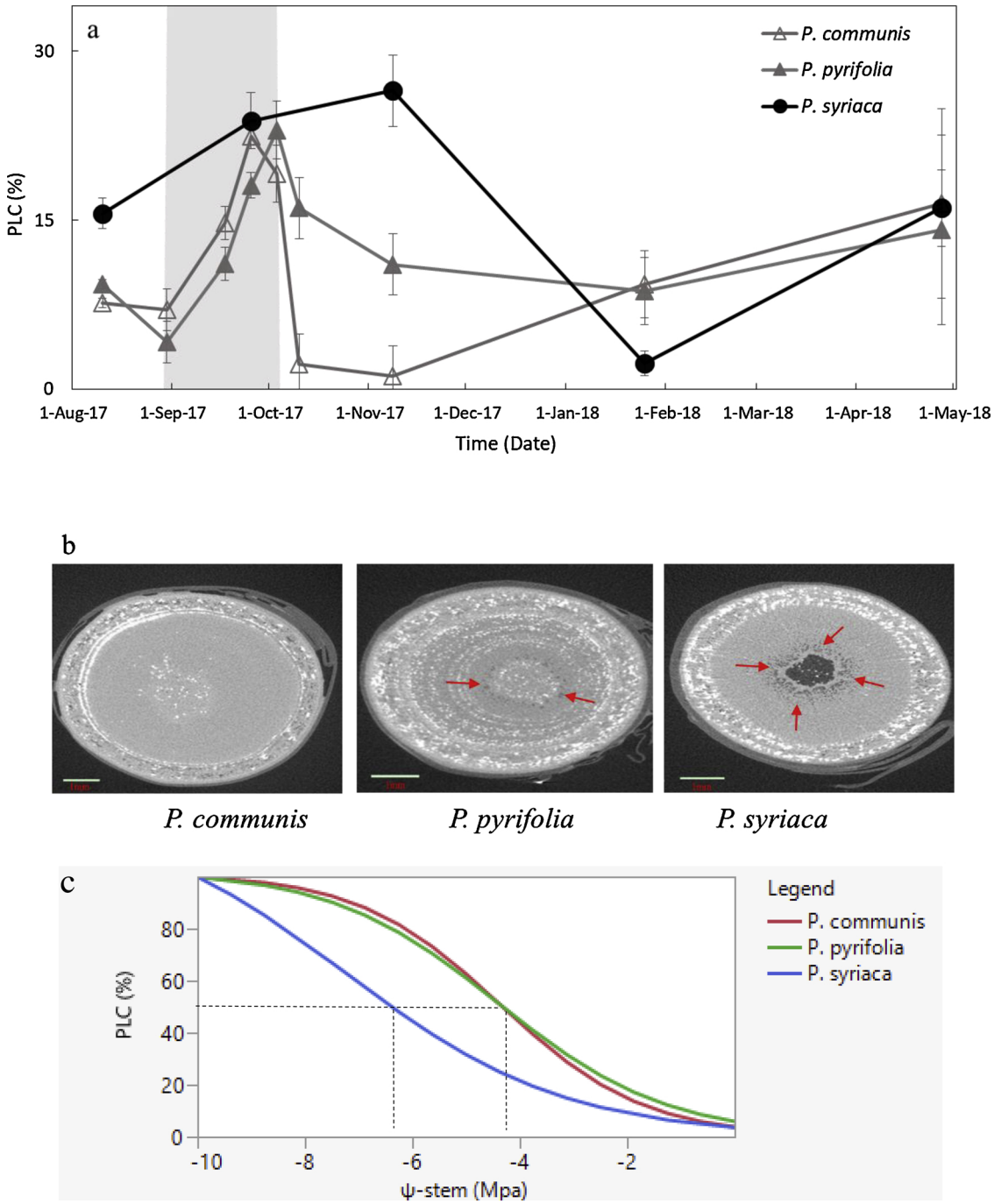

Fig. 5. Percent loss of hydraulic conductivity (PLC; a). Shaded area denotes the 35 days of drought imposed on cultivated trees (*Pyrus communis and Pyrus pyrifolia*). Error bars denote the standard error of the mean ($n = 6$). See Table 1 for statistical analysis. X-ray microtomography (microCT) cross-sections of the embolised vessels (b) in the pear tree branches during recovery (air-filled vessels appear black; denoted by arrows). Xylem vulnerability curves fitted for data-points of each of the three species (c). See Table S3 for curve equations and statistical analysis.

hydraulic traits, leaf gas exchange, PIP mRNA transcription, and non-structural carbohydrate concentrations, suggesting divergent strategies to tolerate drought. Overall, our hypothesis that the wild pear is more drought tolerant than its cultivated counterparts was confirmed. This is because: (1) despite a more negative water potential in the wild pear (Fig. 2a) and its moderate levels of embolism (Fig. 5b), its Kh was less affected by drought than that of the cultivars (Fig. 4a); (2) the latter might be explained by its fewer, narrower vessels (Fig. 6); (3) extrapolating the xylem vulnerability curve based on our PLC measurements indicated a higher drought tolerance (Fig. 5c). Interestingly, the P50 levels estimated for our cultivated and wild trees, −4.3 MPa and −6.4 MPa respectively, were well within the range reported for *Prunus* species (Cochard et al., 2008). However, in that study, some cultivated species showed lower vulnerability to embolism than their wild relatives, related with their drier origin; (4) *P. syriaca* had higher intrinsic water-use efficiency (WUEi) than its cultivated relatives, which had values of 10–30 mmol CO_2 mol^{-1} H_2O, similar to values measured in apple (Regnard et al., 2006). The values of 30–70 mmol CO_2 mol^{-1} H_2O measured in the wild pear were closer to those measured in a broadleaf forest tree such as oak (Klein et al., 2013); and (5) among the three, only the wild species demonstrated a synchronization between starch levels and carbon assimilation rates. Such synchronization is important

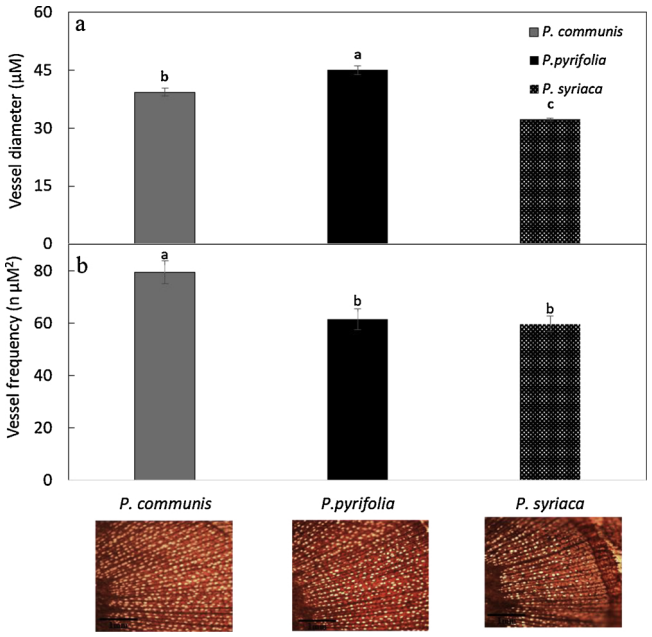

Fig. 6. Mean xylem vessel diameters (a) and frequency of vessels (b) in branches. Means with different lower-case letters are significantly different at *P*-value of 0.05 (Tukey test). Branch cross sections photographed using a digital automated microscope (c).

for storing carbon at high availability, and using reserves at low availability. It is possible that such source-sink relationships have been interfered in the cultivated species due to the stronger fruit sink, which has been the main target of improvement programs. Fruit production has already been shown to act as a strong carbon sink in deciduous trees (Hoch et al., 2002) and specifically in *Pyrus communis* (Naor et al., 2006). Interestingly, interspecific differences in PIP genes expression were relatively small. Still, *P. syriaca* showed a more stable expression pattern of PIP1:1, 1:2, and 1:3 than the other species, where drought-induced downregulation was observed. Among the two cultivars, *P. communis*, but not *P. pyrifolia*, demonstrated responses typically identified with a drought avoidance strategy. This was reflected by its higher levels of NSC (Fig. 8) and higher sensitivity of photosynthesis and transpiration (Fig. 7) indicating higher stomatal regulation. *P. pyrifolia* had higher Kh, a less negative stem WP, higher embolism level, and generally higher downregulation of PIPs under drought (Fig. 4).

Numerous studies have monitored the expression patterns of individual AQP genes in order to elucidate their involvement in plant water relations under mesic and xeric conditions (e.g. Sade et al., 2010, 2014, Secchi and Zwieniecki, 2010, 2013, 2014). Here, a complex gene expression picture was exposed, with large differences between PIP family members, and smaller differences among tree species. This complexity, by itself, suggests multiple cellular functions among the members, potentially in multiple tissue types, which are probably conserved across the studied pear species. Still, stems of all pear trees showed reduction in most PIP gene expression in response to drought (Fig. 4). PIP2:1, 2:2, 2:4 and 2:8 were all strongly downregulated during summer/drought. This expression pattern coincides with a previous report evidencing that AtPIP2:2 and AtPIP2:3 were down-regulated by more than four-fold upon drought stress (Alexandersson et al., 2005). This finding is also in agreement with other studies: measurements in olives showed downregulation of OePIP2:1 expression at the end of a drought period (Perez-Martin et al., 2014). A similar behaviour was also reported by Jang et al. (2004), also showing that *Arabidopsis* PIP2:2 and PIP2:3 were down-regulated following drought stress. These results might indicate a drought response, whereby it is necessary to stop the expression of certain PIP genes, possibly in order to minimize water loss. In contrast, PIP1:1, 1:2, and 1:3 transcripts were still highly expressed in summer in *P. syriaca* (Fig. S1). Moreover, PIP2:6/2:7 and PIP1:4 were upregulated during drought, across the three species. These observations are partly in agreement with previously published reports in other, non-woody species. Alexandersson et al. (2005) reported the upregulation of AtPIP1:4 and AtPIP2:5 in *Arabidopsis*. Furthermore, the expression of PIP1:4 and PIP2:5 is induced under abiotic stress, such as drought conditions, in which the expression of most of the other PIPs is repressed (Kelly et al., 2017). Overexpression of PIP2:5 in seedlings of *Arabidopsis* and of the desert tree species *Tamarix* confers salt and osmotic stress tolerance (Wang et al., 2018). It is therefore possible that these PIPs play a role in the adaptation to drought and help the plant to cope with water stress, potentially by channeling water to target cells. Last, our analysis shows consistently high transcript levels of PIP 1:5/1:6, regardless of the season/treatment, unlike Alexandersson et al. (2005), which instead reported the *Arabidopsis* AtPIP2:6 and AtSIP1:1 to be constitutively expressed and not significantly affected by the drought stress.

Can we link PIP expression patterns to hydraulic changes? In our case this is challenging, since Kh was rather similar (˜1.5–2 Kg MPa^{-1} s^{-1}) across the three species and the two sampling dates (Fig. 4). Still, the two contrasting sampling dates differed significantly in their xylem embolism levels, with ˜17% in summer/drought and only ˜5% in winter/recovery, and in their stem WP levels, with < -1.5 MPa in summer and only -1 MPa in winter. In addition, *P. syriaca* had lower winter PLC, and a more negative summer WP. In a comparison between petiole hydraulics and PIP expression on a sub-diurnal scale, in two grapevine cultivars, VvPIP2:1 and 2:2 responded to WP changes (Shelden et al., 2017). It is hence possible that the differential wild/cultivated pear expression of PIP1:1, 1:2, and 1:3 is related to their WP differences. Paudel et al. (2016) related reductions in root Kh in response to clay soil and treated waste water irrigation with PIP downregulation in *Citrus*. These two recent studies demonstrate how protein water channels, which are cellular components, can respond to, and in turn, also affect, the hydraulic status at the tree level. Therefore, it can well be that the downregulation of nine out of twelve genes studied here is related to the more negative WP and the higher embolism, i.e. as means to minimize water loss at the tree level. In contrast, the drought-induced upregulation of PIP1:4 and PIP2:6/2:7 might indicate an increased water transport to a specific tissue, e.g. to the phloem, to maintain sugar transport under drought, or, presumably, to embolised vessels in the xylem. In *Prunus persica*, a close relative of *Pyrus*, a PIP1 gene upregulation correlated with sugar increase in the bud (Yooyongwech et al., 2009). Although related to chilling, and not drought, tolerance, these results indicated the role of PIP1 in both intra- and intercellular membrane transport, also visually observed with magnetic resonance imaging (Yooyongwech et al., 2008).

In summary, we measured higher drought tolerance in the wild *P. syriaca* than in its most important cultivated relatives, associated with a combination of hydraulic traits (expressed in both xylem anatomy and function), leaf intrinsic water-use efficiency, and carbon management (coordination between photosynthesis and starch levels). In general, *P. syriaca* showed more robust seasonal patterns of photosynthesis, Kh, and PIP expression. Among the cultivars, *P. communis* displayed a drought avoidance strategy, absent in *P. pyrifolia*. The unique study of PIPs in a woody tissue identified a ubiquitous gene (PIP1:5/1:6), nine drought-inhibited genes, and two drought-induced genes (PIP1:4 and 2:6/2:7, confirming previous studies). Due to the time limitation of our experimental system, the need to avoid a risk of affecting fruit production, and high clay soil, 35 days of exposure to drought were used as a representation of a longer-term drought exposure. Yet, stem WP was still significantly higher in the orchard than in the field. Thus, our next research will focus on drought stress in young trees growing in a greenhouse, and will quantify physiological and molecular responses and threshold levels among cultivated and wild pears. Further, we will focus on intensive molecular techniques to test drought tolerance traits of cultivated pears grafted on *P. syriaca* rootstocks, as part of a larger

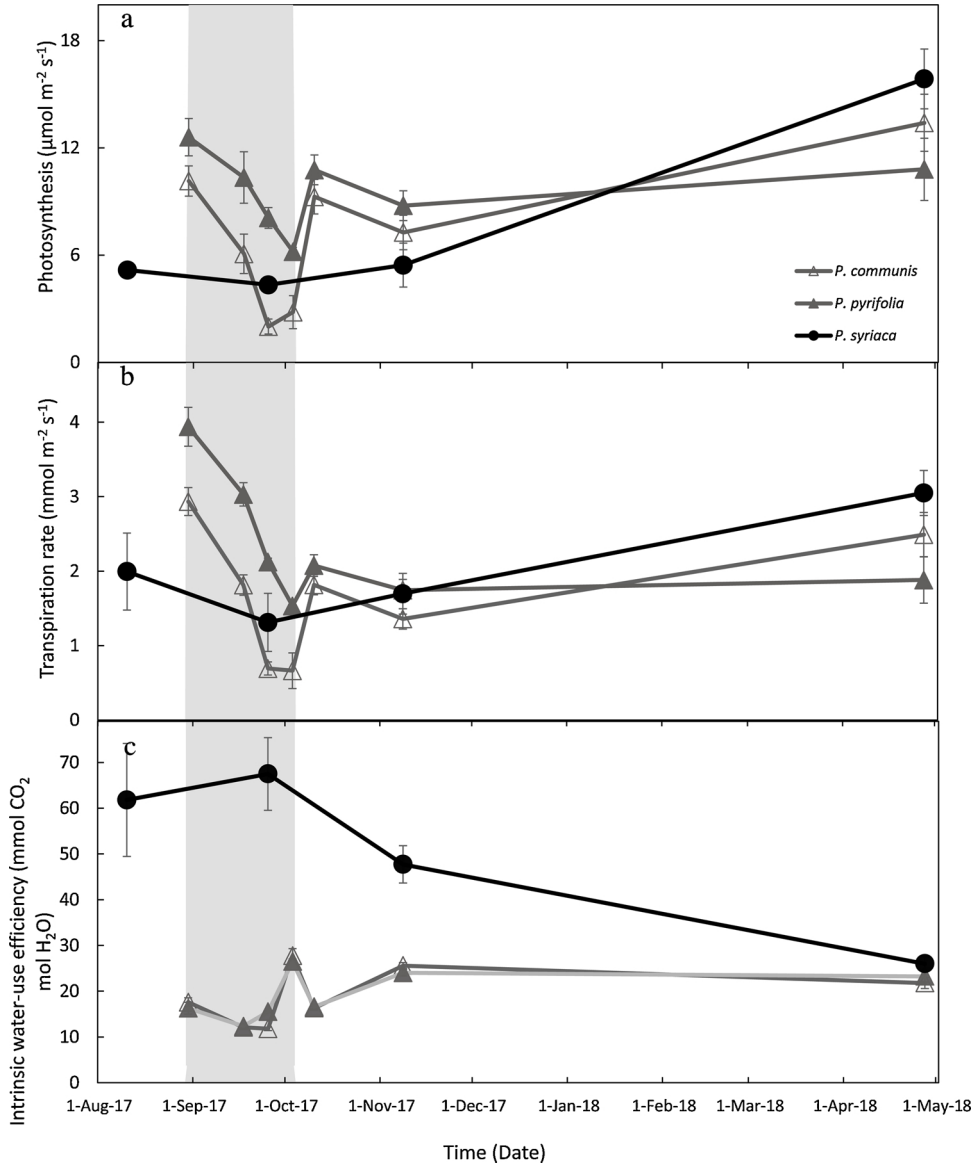

Fig. 7. Photosynthesis (a), Transpiration rate (b), and intrinsic water-use efficiency (c) in the pear trees through the seasons. Shaded area denotes the 35 days of drought imposed on cultivated trees (*Pyrus communis and Pyrus pyrifolia*). Error bars denote the standard error of the mean ($n = 6$). See Table 1 for statistical analysis.

project of preparing fruit orchards for the future climate. In addition, we have started exploring tissue localization, function, and structural differences among the pear PIPs, focusing on PIP1:4 and 2:6/2:7, which presented drought-induced upregulation, and the *P. syriaca* PIP1:1, 1:2, and 1:3, which were kept at normal expression level despite the drought. Finally, this study used the eco-physiological definition of tree drought tolerance, i.e. tree survival and growth, rather than the agricultural definition, which is defined by the yield penalty. The higher gas exchange activity and photosynthesis, at a wider water potential range, in the wild vs. the cultivated pears, presents a good potential for further testing in an agricultural framework.

Author contributions

IP coordinated the measurements and most of the analysis and provided the first draft; HG helped in the measurements and in writing the manuscript; TK initiated the project, designed the experiment, and wrote the manuscript; AZ and GS helped in coordinating the field sites; SBD defined the aquaporin genes and designed the primers; and VB consulted the microCT scans.

Acknowledgments

IP wishes to thank to the Weizmann Prestigious Dean Fellowship program. TK wishes to thank Orna Reisman-Berman of the Ben Gurion University of the Negev for her help in developing the research idea; and Menachem Moshelion of the Hebrew University of Jerusalem and David Granot of the ARO Volcani center for critical reading of an earlier version of the paper. The project was funded in part by the Merle S. Cahn Foundation and the Monroe and Marjorie Burk Fund for Alternative Energy Studies; Mr. and Mrs. Norman Reiser, together with the Weizmann Center for New Scientists; The Yeda-Sela Center for Basic Research; and the Edith & Nathan Goldberg Career Development Chair. The authors declare no conflict of interest.

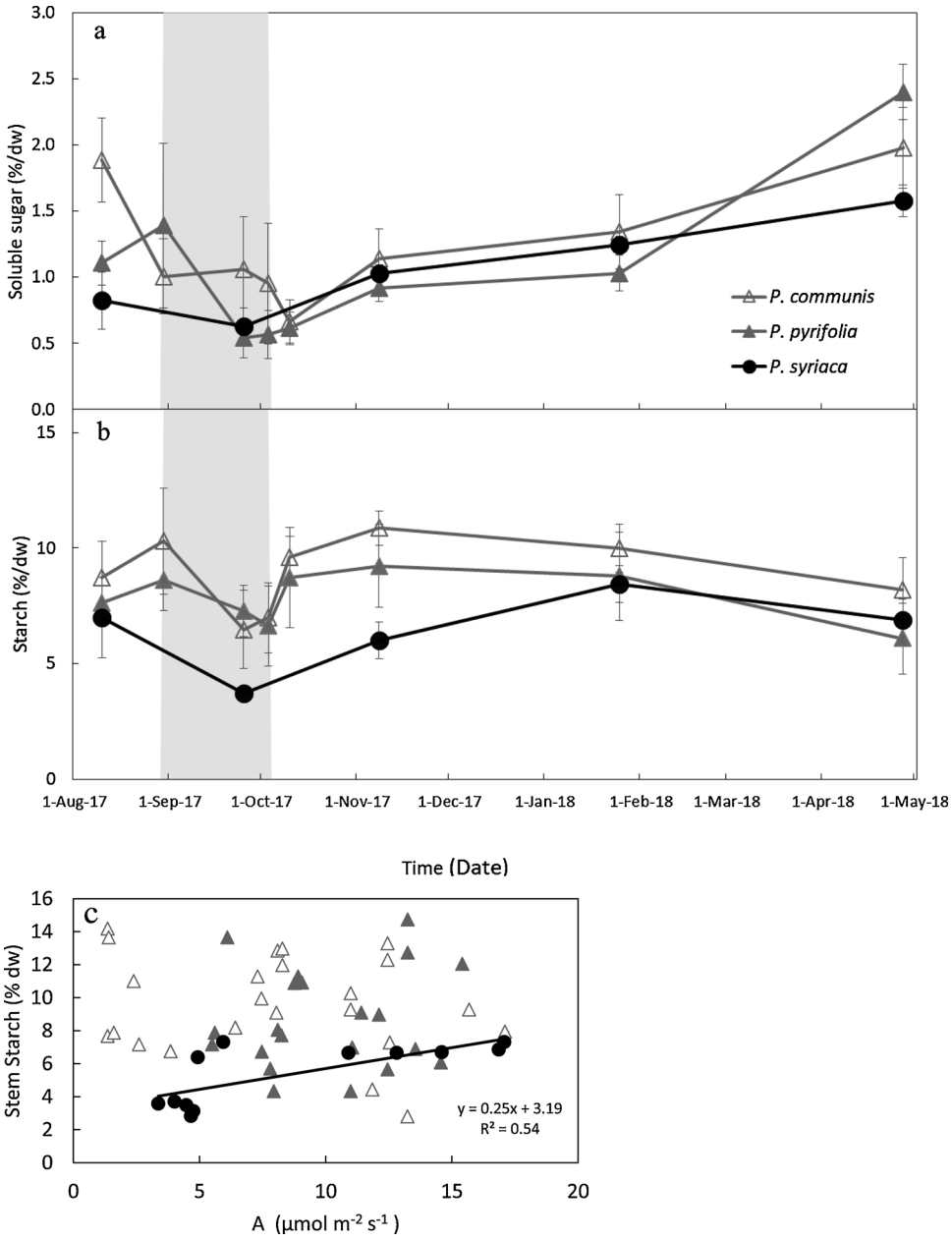

Fig. 8. Stem soluble sugar (a) and starch content (b) in pear branches through the seasons. Shaded area denotes the 35 days of drought imposed on cultivated trees (*Pyrus communis and Pyrus pyrifolia*). Error bars denote the standard error of the mean (n = 6). See Table 1 for statistical analysis. Relationship between stem starch content and net assimilation (c) for the three species, with linear regression for *P. syriaca*, where regression was statistically significant.

Appendix A. Supplementary data

Supplementary material related to this article can be found, in the online version, at doi:https://doi.org/10.1016/j.envexpbot.2019.103832.

References

Alexandersson, E., Fraysse, L., Sjövall-Larsen, S., Gustavsson, S., Fellert, M., Karlsson, M., Kjellbom, P., 2005. Whole gene family expression and drought stress regulation of aquaporins. Plant Mol. Biol. 59 (3), 469–484.

Almeida-Rodriguez, A.M., Hacke, U.G., 2012. Cellular localization of aquaporin mRNA in hybrid poplar stems. Am. J. Bot. 99 (7), 1249–1254. https://doi.org/10.3732/ajb.1200088.

Aroca, R., Porcel, R., Ruiz-Lozano, J.M., 2012. Regulation of root water uptake under abiotic stress conditions. J. Exp. Bot. 63 (1), 43–57.

Beikircher, B., Mayr, S., 2016. Avoidance of harvesting and sampling artefacts in hydraulic analyses: a protocol tested on *Malus domestica*. Tree Physiol. 36 (6), 797.

Brodersen, C.R., McElrone, A.J., Choat, B., Lee, E.F., Shackel, K.A., Matthews, M.A., 2013. In vivo visualizations of drought-induced embolism spread in *Vitis vinifera*. Plant Physiol. 161, 1820–1829.

Brodribb, T.J., Holbrook, N.M., 2003. Stomatal closure during leaf dehydration, correlation with other leaf physiological traits. Plant Physiol. 132 (4), 2166–2173.

Brodribb, T.J., McAdam, S.A., 2017. Evolution of the stomatal regulation of plant water content. Plant Physiol. 174 (2), 639–649.

Cochard, H., Barigah, S.T., Kleinhentz, M., Eshel, A., 2008. Is xylem cavitation resistance a relevant criterion for screening drought resistance among *Prunus species*? J. Plant Physiol. 165 (9), 976–982.

Degu, H.D., Adur, U., Shatil-Cohen, A., Moshelion, J.D.K.M., Cohen, Y., 2013. Date-palm aquaporins PdPIP1; 1 and PdPIP1; 3 are involved in early drought stress response. World Acad. Sci. Eng. Technol. 79, 1403–1410.

Deshmukh, R.K., Vivancos, J., Ramakrishnan, G., Guérin, V., Carpentier, G., Sonah, H., et al., 2015. A precise spacing between the NPA domains of aquaporins is essential for silicon permeability in plants. Plant J. 83 (3), 489–500.

Feinbrun-Dothan, N., Danin, A., 1991. Analytical Flora of the Land of Israel. Cana, Jerusalem. .

Feurtey, A., Cornille, A., Shykoff, J.A., Snirc, A., Giraud, T., 2017. Crop-to-wild gene flow and its fitness consequences for a wild fruit tree: towards a comprehensive conservation strategy of the wild apple in Europe. Evol. Appl. 10 (2), 180–188.

Gambetta, G.A., Fei, J., Rost, T.L., Knipfer, T., Matthews, M.A., Shackel, K.A., McElrone, A.J., 2013. Water uptake along the length of grapevine fine roots: developmental anatomy, tissue-specific aquaporin expression, and pathways of water transport. Plant Physiol. 163 (3), 1254–1265.

Han, Q., Kabeya, D., Hoch, G., 2011. Leaf traits, shoot growth and seed production in mature *Fagus sylvatica* trees after 8 years of CO_2 enrichment. Ann. Bot. 107 (8), 1405–1411.

Hoch, G., Popp, M., Körner, C., 2002. Altitudinal increase of mobile carbon pools in Pinus cembra suggests sink limitation of growth at the Swiss treeline. Oikos 98 (3), 361–374.

Jang, J.Y., Kim, D.G., Kim, Y.O., Kim, J.S., Kang, H., 2004. An expression analysis of a gene family encoding plasma membrane aquaporins in response to abiotic stresses in *Arabidopsis thaliana*. Plant Mol. Biol. 54 (5), 713–725.

Kelly, G., Sade, N., Doron-Faigenboim, A., Lerner, S., Shatil-Cohen, A., Yeselson, Y., Granot, D., 2017. Sugar and hexokinase suppress expression of PIP aquaporins and reduce leaf hydraulics that preserves leaf water potential. Plant J. 91 (2), 325–339.

Klein, T., Cohen, S., Yakir, D., 2011. Hydraulic adjustments underlying drought resistance of *Pinus halepensis*. Tree Physiol. 31 (6), 637–648.

Klein, T., Randin, C., Körner, C., 2015. Water availability predicts forest canopy height at the global scale. Ecol. Lett. 18 (12), 1311–1320.

Klein, T., Shpringer, I., Fikler, B., Elbaz, G., Cohen, S., Yakir, D., 2013. Relationships between stomatal regulation, water-use, and water-use efficiency of two coexisting key Mediterranean tree species. For. Ecol. Manage. 302, 34–42.

McDowell, N., Pockman, W.T., Allen, C.D., Breshears, D.D., Cobb, N., Kolb, T., et al., 2008. Mechanisms of plant survival and mortality during drought: why do some plants survive while others succumb to drought? New Phytol. 178 (4), 719–739.

Mund, M., Kutsch, W.L., Wirth, C., Kahl, T., Knohl, A., Skomarkova, M.V., Schulze, E.D., 2010. The influence of climate and fructification on the inter-annual variability of stem growth and net primary productivity in an old-growth, mixed beech forest. Tree Physiol. 30 (6), 689–704.

Naor, A., Stern, R., Flaishman, M., Gal, Y., Peres, M., 2006. Effects of post-harvest water stress on autumnal bloom and subsequent-season productivity in mid-season 'Spadona'pear. J. Hortic. Sci. Biotechnol. 81 (3), 365–370.

Nardini, A., Gullo, M.A.L., Salleo, S., 2011. Refilling embolized xylem conduits: is it a matter of phloem unloading? Plant Sci. 180 (4), 604–611.

Paudel, I., Cohen, S., Shlizerman, L., Jaiswal, A.K., Shaviv, A., Sadka, A., 2017. Reductions in root hydraulic conductivity in response to clay soil and treated waste water are related to PIPs down-regulation in Citrus. Sci. Rep. 7 (1), 15429.

Paudel, I., Cohen, S., Shaviv, A., Bernstein, N., Heuer, B., Bar-Tal, A., Ephrath, J., 2016. Impact of treated wastewater on growth, respiration, and hydraulic conductivity of citrus root systems in light and heavy soils. Tree Physiol.

Perez-Martin, A., Michelazzo, C., Torres-Ruiz, J.M., Flexas, J., Fernández, J.E., Sebastiani, L., Diaz-Espejo, A., 2014. Regulation of photosynthesis and stomatal and mesophyll conductance under water stress and recovery in olive trees: correlation with gene expression of carbonic anhydrase and aquaporins. J. Exp. Bot. 65 (12), 3143–3156.

Pockman, W.T., Sperry, J.S., 2000. Vulnerability to xylem cavitation and the distribution of Sonoran desert vegetation. Am. J. Bot. 87 (9), 1287–1299.

Prado, K., Boursiac, Y., Tournaire-Roux, C., Monneuse, J.M., Postaire, O., Da Ines, O., et al., 2013. Regulation of Arabidopsis leaf hydraulics involves light-dependent phosphorylation of aquaporins in veins. Plant Cell 25 (3), 1029–1039.

Reales, A., Sargent, D.J., Tobutt, K.R., Rivera, D., 2010. Phylogenetics of *Eurasian plums*, Prunus L. section Prunus (Rosaceae), according to coding and non-coding chloroplast DNA sequences. Tree Genet. Genomes 6 (1), 37–45.

Paudel, I., Halpern, M., Wagner, Y., Raveh, E., Yermiyahu, U., Hoch, G., Klein, T., 2018. Elevated CO_2 compensates for drought effects in lemon saplings via stomatal downregulation, increased soil moisture, and increased wood carbon storage. Environ. Exp. Bot. 148, 117–127.

Prendin, A.L., Petit, G., Carrer, M., Fonti, P., Björklund, J., von Arx, G., 2017. New research perspectives from a novel approach to quantify tracheid wall thickness. Tree Physiol. 37 (7), 976–983.

Regnard, J.L., Ducrey, M., Porteix, E., Segura, V., Costes, E., 2006. August). Phenotyping apple progeny for ecophysiological traits: how and what for? XXVII International Horticultural Congress-IHC2006: International Symposium on Enhancing Economic and Environmental 772, 151–158.

Romero, P., Botía, P., 2006. Daily and seasonal patterns of leaf water relations and gas exchange of regulated deficit-irrigated almond trees under semiarid conditions. Environ. Exp. Bot. 56 (2), 158–173.

Sade, N., Gallé, A., Flexas, J., Lerner, S., Peleg, G., Yaaran, A., Moshelion, M., 2014. Differential tissue-specific expression of NtAQP1 in Arabidopsis thaliana reveals a role for this protein in stomatal and mesophyll conductance of CO_2 under standard and salt-stress conditions. Planta 239 (2), 357–366.

Sade, N., Gebretsadik, M., Seligmann, R., Schwartz, A., Wallach, R., Moshelion, M., 2010. The role of tobacco Aquaporin1 in improving water use efficiency, hydraulic conductivity, and yield production under salt stress. Plant Physiol. 152 (1), 245–254.

Schröder, R., Prasse, R., 2013. Do cultivated varieties of native plants have the ability to outperform their wild relatives? PLoS One 8 (8), e71066.

Secchi, F., Zwieniecki, M.A., 2010. Patterns of PIP gene expression in Populus trichocarpa during recovery from xylem embolism suggest a major role for the PIP1 aquaporin subfamily as moderators of refilling process. Plant Cell Environ. 33 (8), 1285–1297.

Secchi, F., Zwieniecki, M.A., 2013. The physiological response of Populus tremula x alba leaves to the down-regulation of PIP1 aquaporin gene expression under no water stress. Front. Plant Sci. 4, 507. https://doi.org/10.3389/fpls.2013.00507.

Secchi, F., Zwieniecki, M.A., 2014. Down-regulation of plasma intrinsic protein1 aquaporin in poplar trees is detrimental to recovery from embolism. Plant Physiol. 164 (4), 1789–1799. https://doi.org/10.1104/pp.114.237511.

Shelden, M.C., Vandeleur, R., Kaiser, B.N., Tyerman, S.D., 2017. A comparison of petiole hydraulics and aquaporin expression in an anisohydric and isohydric cultivar of grapevine in response to water-stress induced cavitation. Front. Plant Sci. 8, 1893.

Sperry, J.S., Donnelly, J.R., Tyree, M.T., 1988. A method for measuring hydraulic conductivity and embolism in xylem. Plant Cell Environ. 11 (1), 35–40.

Tyree, M.T., Zimmermann, M.H., 2002. Hydraulic architecture of whole plants and plant performance. Xylem Structure and the Ascent of Sap. Springer, Berlin Heidelberg, pp. 175–214.

Tyree, M.T., Patiño, S., Bennink, J., Alexander, J., 1995. Dynamic measurements of roots hydraulic conductance using a high-pressure flowmeter in the laboratory and field. J. Exp. Bot. 46 (1), 83–94.

Vilagrosa, A., Morales, F., Abadía, A., Bellot, J., Cochard, H., Gil-Pelegrin, E., 2010. Are symplast tolerance to intense drought conditions and xylem vulnerability to cavitation coordinated? An integrated analysis of photosynthetic, hydraulic and leaf level processes in two Mediterranean drought-resistant species. Environ. Exp. Bot. 69 (3), 233–242.

Von Arx, G., Carrer, M., 2014. ROXAS–a new tool to build centuries-long tracheid-lumen chronologies in conifers. Dendrochronologia 32 (3), 290–293.

Von Arx, G., Dietz, H., 2005. Automated image analysis of annual rings in the roots of perennial forbs. Int. J. Plant Sci. 166 (5), 723–732.

Wang, L., Zhang, C., Wang, Y., Wang, Y., Yang, C., Lu, M., Wang, C., 2018. Tamarix hispida aquaporin ThPIP2; 5 confers salt and osmotic stress tolerance to transgenic Tamarix and Arabidopsis. Environ. Exp. Bot. 152, 158–166.

Wheeler, J.K., Huggett, B.A., Tofte, A.N., Rockwell, F.E., Holbrook, N.M., 2013. Cutting xylem under tension or supersaturated with gas can generate PLC and the appearance of rapid recovery from embolism. Plant Cell Environ. 36 (11), 1938–1949.

Wong, S.C., 1990. Elevated atmospheric partial pressure of CO 2 and plant growth. Photosyn. Res. 23 (2), 171–180.

Yooyongwech, S., Horigane, A.K., Yoshida, M., Yamaguchi, M., Sekozawa, Y., Sugaya, S., Gemma, H., 2008. Changes in aquaporin gene expression and magnetic resonance imaging of water status in peach tree flower buds during dormancy. Physiol. Plant. 134 (3), 522–533.

Yooyongwech, S., Sugaya, S., Sekozawa, Y., Gemma, H., 2009. Differential adaptation of high-and low-chill dormant peaches in winter through aquaporin gene expression and soluble sugar content. Plant Cell Rep. 28 (11), 1709.

Zohary, D., 1972. The wild progenitor and the place of origin of the cultivated lentil: *Lens culinaris*. Econ. Bot. 26 (4), 326–332.

Zwieniecki, M.A., Secchi, F., 2017. Role of aquaporins in the maintenance of xylem hydraulic capacity. Plant Aquaporins. Springer International Publishing, pp. 237–254.